2011 3rd International Conference on Signal Processing Systems (ICSPS 2011)
IPCSIT vol. 48 (2012) © (2012) IACSIT Press, Singapore
DOI: 10.7763/IPCSIT.2012.V48.12

A Real-time Photoacoustic Imaging System with High Density Integrated Circuit

Naizhang Feng*, Mingjian Sun and Liyong Ma

Department of Control Science and Engineering, Harbin Institute of Technology, Harbin 150001, China
*Email: fengnz@yeah.net

Abstract. Based on an array transducer, a real-time photoacoustic imaging system with high density integrated circuit is built. The system is composed of a short pulsed laser, an ultrasonic transducer array, a data acquisition circuit and a computer. The data acquisition circuit consists of 128-channel variable gain amplifiers, 128-channel anti-aliasing filters, 128-channel analog-to-digital converters, and field programmable gate arrays. Biological tissues are irradiated by the laser to generate the thermoelastic expansion. The transducer array is used to detect the photoacoustic signals generated from the tissue thermoelastic expansion. Then the photoacoustic signals are amplified and sampled by multiple parallel data acquisition channels. Subsequently, the sampled data set is transferred to the computer through an USB interface. The final photoacoustic image is reconstructed by the computer. The traditional "delay-and-sum" beamforming method is used as the reconstruction algorithm. An experiment with a phantom of two hairs is made. The result shows that two hairs can be displayed clearly in the reconstructed image and the imaging rate is the same as the pulse repetition frequency of the laser.

Keywords: Photoacoustic Imaging; Real time; Data acquisition Channel; Beamforming

1. Introduction

As a new technique, photoacoustic imaging (PAI) for biological tissues has been proposed and developed in recent years[1,2]. It has demonstrated great potential for visualization of the internal structures and function of soft tissue. When biological tissues are irradiated by a short pulsed laser, some energy is absorbed to generate the transient thermoelastic expansion. The expansion leads to a wideband ultrasonic emission. The generated ultrasonic waves are then detected by ultrasonic transducers to form images[3-5]. PA images combine high ultrasonic penetration and strong optical contrast in a single modality.

For the scanning PAI system, hundreds or even thousands of scanning steps are required to form an image[6]. The scanning process usually takes several minutes and the long acquisition time will lead to movement artifacts. To realize the real-time imaging, an ultrasonic transducer array can be used to detect the PA signals[7-10]. For the PAI system based on an ultrasonic transducer array, a large number of parallel data acquisition (DAQ) channels are needed. In order to decrease the system cost and complexity, a real-time PA imaging system with high density integrated circuit is constructed in this paper.

2. Photoacoustic Imaging System

The system diagram is illustrated in Figure 1, which is composed of a short pulsed laser, an ultrasonic transducer array, a data acquisition (DAQ) circuit and a computer. The laser transmits 7 ns pulses to irradiate the biological tissues at 15 Hz with wavelength 532nm. The transducer array (L10-5, 38 mm, 128 elements, 7.5-MHz central frequency, 75% -6dB bandwidth) is used to detect the PA signals generated from the tissue thermoelastic expansion. Then the PA signals are amplified and sampled by multiple parallel DAQ channels.

Subsequently, the sampled data set is transferred to the computer through an USB interface. The final PA image is reconstructed by the computer.

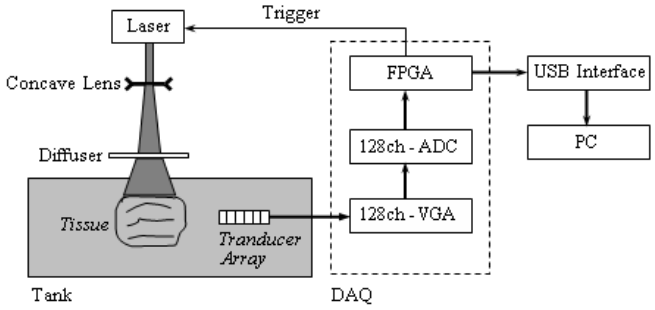

Fig.1. Diagram of photoacoustic imaging system

The data acquisition circuit includes 128 DAQ channels, which are composed of variable gain amplifiers (VGA), analog-to-digital converters (ADC) and field programmable gate arrays (FPGA). The specific chips include AD9272 and EP3C55.

The chip AD9272 contains eight channels of a low noise preamplifier (LNA) with a VGA, an anti-aliasing filter (AAF), and a 12-bit, 10 MSPS to 80 MSPS ADC[11]. Its internal structure is illustrated in Figure 2. It is designed for low cost, low power, small size, and ease of use. Good noise performance relies on a proprietary ultra-low noise LNA at the beginning of the signal chain, which minimizes the noise contribution in the following VGA. Active impedance control optimizes noise performance for applications that benefit from input impedance matching. The anti-aliasing filter that the signal reaches prior to the ADC is used to reject dc signals and to band limit the signal for anti-aliasing. AD9272 uses a pipelined ADC architecture. The quantized output from each stage is combined into a 12-bit result in the digital correction logic. The pipelined architecture permits the first stage to operate on a new input sample and the remaining stages to operate on preceding samples. Sampling occurs on the rising edge of the clock. The ADC LVDS (Low Voltage Differential Signaling) outputs facilitate interfacing with LVDS receivers in custom ASICs (Application Specific Integrated Circuit) and FPGAs that have LVDS capability for superior switching performance in noisy environments. Here, two FPGAs are adopted to interface with ADCs and each FPGA records the data of 64 DAQ channels.

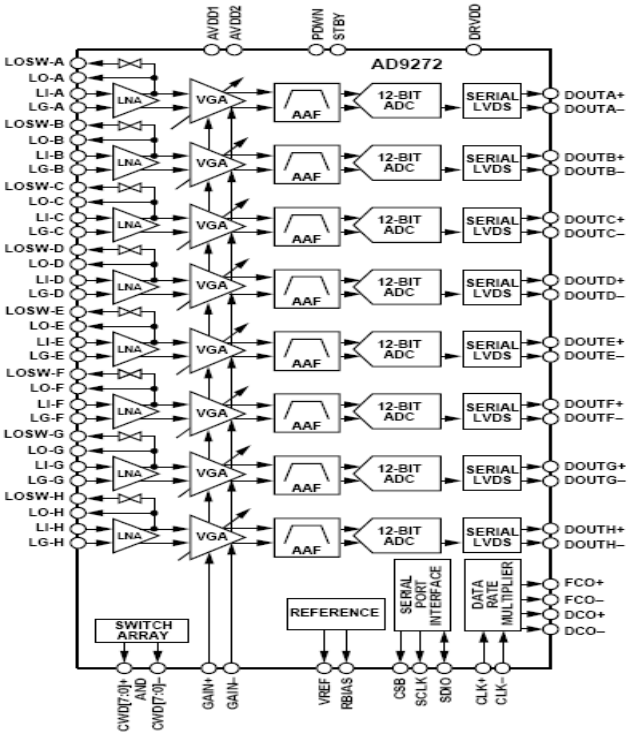

Fig.2. Functional block diagram of AD9272

EP3C55 is a FPGA chip of Cyclone III series made by Altera Incorporation[12]. Cyclone III device family includes a customer-defined feature set that is optimized for portable applications and offers a wide range of density, memory, embedded multiplier, and I/O options. Cyclone III device family provides the ideal solution for your high-volume, low-power, and cost-sensitive applications. EP3C55 owns 55,856 logic elements and 260 distributed memory blocks. The logic array block (LAB) consists of 16 logic elements and a LAB-wide control block. An LE is the smallest unit of logic in the Cyclone III device family architecture. Each LE has four inputs, a four-input look-up table (LUT), a register, and output logic. The four-input LUT is a function generator that can implement any function with four variables. Each memory block provides nine Kbits of on-chip memory capable of operating at up to 315 MHz. The embedded memory structure consists of M9K memory blocks columns that you can configure as RAM, first-in first-out (FIFO) buffers, or ROM. The ADC sampling rate is set to 40 MHz. Four memory blocks (buffer length is 1k×12bit) are used to record a DAQ channel data with maximum depth 4cm. Thus, 64 DAQ channels occupy 256 memory blocks.

CY7C68013 is an USB interface chip with USB 2.0 protocol[13]. CY7C68013 fabricates 4KB FIFO to provide a high speed data transfer with 96 MBytes/s burst rate. The PA signals are sampled and recorded in distributed memory blocks. Then the distributed data sets are collected and transferred to the FIFO of CY7C68013, which is shown in Figure 3. At the same time, CY7C68013 reads data from the FIFO and transfer them to the internal memory of the computer. The total data volume of a frame image is 2(FPGA)×256(block)×512(Byte/block)=256KB. The pulse repetition frequency of the laser is 15Hz. To achieve the maximum imaging frame rate, it is necessary to transfer 256KB×15=1.25MB data per second. It is easy to attain since CY7C68013 can transfer more than 20MB data per second usually.

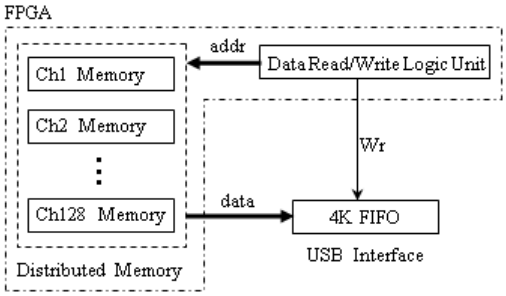

Fig.3. Diagram of data transfer

Based on the above description, the system hardware is built and shown in Figure 4.

Fig.4. Picture of the photoacoustic imaging system

In order to realize the real time imaging, a fast speed reconstruction algorithm is required. The beamforming method is an alternative one.

3. Photoacoustic Image Reconstruction

In PAI, when the pulsed laser irradiates the testing tissue, the light quickly spreads throughout the tissue due to scattering. Therefore, the PA response is simultaneously produced everywhere in the tissue. All transducer elements are used to receive the PA signals at once. Based on the received data, every scan line can be reconstructed quickly by the traditional “delay-and-sum” beamforming method [14,15], shown in Figure 5. At the center of the transducer, the focusing aperture is symmetrical, shown in Figure 6. At the

edge of the transducer, the focusing aperture is asymmetrical, shown in Figure 7. The asymmetry of the focusing aperture can lead to the sidelobe rise.

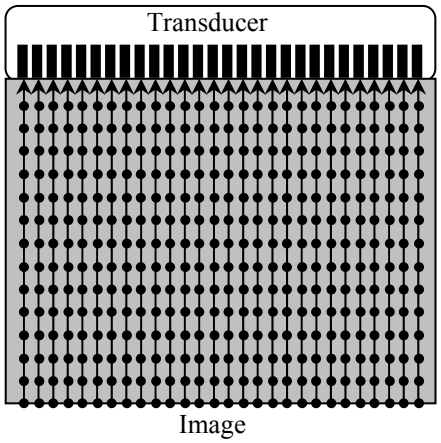

Fig.5. Image reconstruction based on beamforming

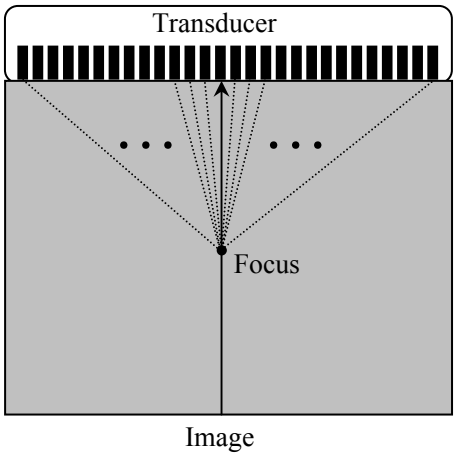

Fig.6. Focusing schematic at the center of the transducer

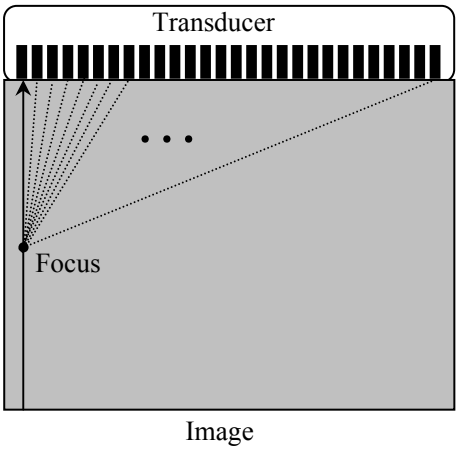

Fig.7. Focusing schematic at the edge of the transducer

In order to improve the contrast resolution of the reconstructed image, the apodization weighting technology should be applied. Different weightings are selected for different scan lines to balance the lateral resolution of the reconstructed image. The apodization weighting curves at the edge and center of the transducer are plotted in Figure 8(a), and the corresponding beam patterns are plotted in Figure 8(b). It is seen that the mainlobes are comparable, while the sidelobe level at the edge of the transducer is obviously higher than that at the center of the transducer. As a result, the contrast resolution at the edge of the reconstructed image is worse than that at the center.

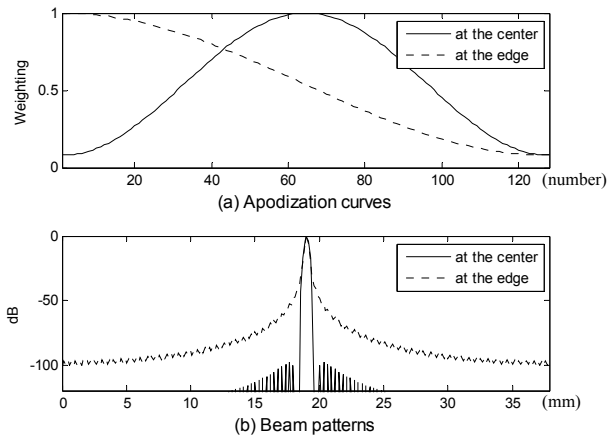

Fig.8. Apodization and beam pattern

The focusing delay parameters can be computed in advance and the focus data can be indexed quickly by the focusing delay parameters. Then, the focus points of multi-channels are weighted and accumulated. Since the "delay-and-sum" beamforming algorithm has no complex computation, the PA image can be reconstructed in real time by the algorithm.

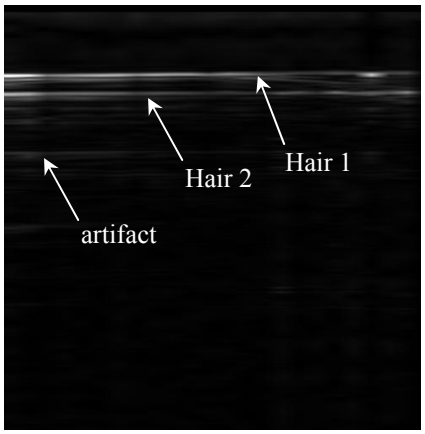

Fig.9. The experiment result of a two hair phantom

An experiment is made based on the constructed hardware platform shown in Figure 4. The phantom of two hairs is irradiated by the short-pulsed laser. The generated PA signals are detected by the array transducer. Then they are amplified, sampled and transferred to the computer. The PA image is reconstructed on the computer and shown in Figure 9. From the experiment result, it is seen that the two hairs can be detected and displayed clearly. Also, some artifacts are displayed in the image, which are caused by the multiple reflections of the PA signals from the transducer surface. The imaging rate is the same as the pulse repetition frequency of the laser.

4. Conclusion

In order to decrease the system cost and complexity, a real-time photoacoustic imaging system with high density integrated circuit is built in this paper. The system consists of a short pulsed laser, an ultrasonic transducer array, a data acquisition circuit and a computer. The data acquisition circuit includes 128 high integrated channels which is composed of 128 LNAs, 128 VGAs, 128 ADCs and 2 FPGAs. As a result, the PA signals can be detected by 128 transducer elements simultaneously. Subsequently, the sampled data set is transferred to the computer through an USB interface. The final PA image is reconstructed by the computer. The traditional "delay-and-sum" beamforming method is used to reconstruct the PA image quickly. The imaging rate can attain to the pulse repetition frequency of the laser. Based on the built system platform, an experiment with a phantom of two hairs is made. The result shows that two hairs can be displayed clearly in the reconstructed image. However, some artifacts are still displayed in the image, which are caused by the multiple reflections of the PA signals from the transducer surface.

5. Acknowledgment

This work is supported by the National Natural Science Foundation of China (No. 30800240), Shandong Provincial Promotive Research Fund for Excellent Young and Middle-aged Scientists (BS2010DX001) and Weihai City Science & Technology Development Project (2010-3-96).

6. References

[1] L. V. Wang, "Prospects of photoacoustic tomography," Medical Physics, vol.35, no.12, 2008, pp. 5759-5767.

[2] Z. Xu, C. Li, L. V. Wang, "Photoacoustic tomography of water in phantoms and tissue," Journal of Biomedical Optics, vol.13, no.3, 2010, pp.036019:1-6.

[3] B. E. Treeby, B. T. Cox, "k-Wave: MATLAB toolbox for the simulation and reconstruction of photoacoustic wave fields," Journal of Biomedical Optics, vol.15, no.2, 2010, pp.021314:1-12.

[4] H. F. Zhang, K. Maslov, G. Stoica, et al, “Functional photoacoustic microscopy for high-resolution and noninvasive in vivo imaging. Nature Biotechnology,” vol.24, no.7, 2006, pp.848-851.

[5] M. Xu, L. V. Wang, “Photoacoustic imaging in biomedicine,” Review of Scientific Instruments, vol.77, 2006, pp.041101:1-21.

[6] Z. Guo, C. Li, L. Song, et al, “Compressed sensing in photoacoustic tomography in vivo,” Journal of Biomedical Optics, vol.15, no.2, 2010, pp.021311:1-6.

[7] J. J. Niederhauser, M. Jaeger, R. Lemor, et al, “Combined ultrasound and ptoacoustic system for real-time high-contrast vascular imaging in vivo,” IEEE Trans. Med. Imag., vol.24, no.4, 2005, pp.436-440

[8] Y. Zeng, D. Xing, Y. Wang, et al, “Photoacoustic and ultrasonic coimage with a linear transducer array,” Opt. Lett., vol.29, no.15, 2004, pp.1760-1762

[9] S. Park, S. Mallidi, A. B. Karpiouk, et al, “Photoacoustic imaging using array transducer,” Proc. of SPIE, vol.6437, 2007, pp.643714:1-7

[10] R. G. M. Kolkman, P. J. Brands, W. Steenbergen, et al, “Real-time in vivo photoacoustic and ultrasound imaging,” Journal of Biomedical Optics, vol.13, no.5, 2008, pp. 050510:1-3.

[11] “AD9272-Octal LNA/VGA/AAF/ADC and Crosspoint Switch Datasheet,” 2009, Analog Devices Incorporation.

[12] “Cyclone III Device Handbook,” 2009, Altera Corporation.

[13] “CY7C68013 EZ-USB FX2™ USB Microcontroller High-speed USB Peripheral Controller Datasheet,” 2002, Cypress Semiconductor Corporation.

[14] S. Park, S. R. Aglyamov, S. Y. Emelianov, “Beamforming for photoacoustic imaging using linear array transducer,” IEEE Ultrasonics Symposium, 2007, pp.856-859

[15] S. Park, A. B. Karpiouk, S. R. Aglyamov, et al, “Adaptive beamforming for photoacoustic imaging using linear array transducer,” IEEE Ultrasonics Symposium, 2008, pp.1088-1091